HHS Public Access

Author manuscript

Cell Rep. Author manuscript; available in PMC 2018 November 21.

Published in final edited form as:

Cell Rep. 2016 November 08; 17(7): 1807–1818. doi:10.1016/j.celrep.2016.10.044.

A Small Potassium Current in AgRP/NPY Neurons Regulates Feeding Behavior and Energy Metabolism

Yanlin He[1,6], **Gang Shu**[1,2,6], **Yongjie Yang**[1], **Pingwen Xu**[1], **Yan Xia**[1], **Chunmei Wang**[1], **Kenji Saito**[1], **Antentor Hinton Jr.**[1], **Xiaofeng Yan**[1], **Chen Liu**[3], **Qi Wu**[1], **Qingchun Tong**[4], and **Yong Xu**[1,5,7,*]

[1]Children's Nutrition Research Center, Department of Pediatrics, Baylor College of Medicine, One Baylor Plaza, Houston, TX 77030, USA

[2]College of Animal Science, South China Agricultural University, Guangzhou 100044, China

[3]Division of Hypothalamic Research, Department of Internal Medical, University of Texas Southwestern Medical Center, Dallas, TX 75390, USA

[4]Brown Foundation Institute of Molecular Medicine, University of Texas Health Science Center at Houston, Houston, TX 77030, USA

[5]Department of Molecular and Cellular Biology, Baylor College of Medicine, One Baylor Plaza, Houston, TX 77030, USA

[6]Co-first author

[7]Lead Contact

SUMMARY

Neurons that co-express agouti-related peptide (AgRP) and neuropeptide Y (NPY) are indispensable for normal feeding behavior. Firing activities of AgRP/NPY neurons are dynamically regulated by energy status and coordinate appropriate feeding behavior to meet nutritional demands. However, intrinsic mechanisms that regulate AgRP/NPY neural activities during the fed-to-fasted transition are not fully understood. We found that AgRP/NPY neurons in satiated mice express high levels of the small-conductance calcium-activated potassium channel 3 (SK3) and are inhibited by SK3-mediated potassium currents; on the other hand, food deprivation suppresses SK3 expression in AgRP/NPY neurons, and the decreased SK3-mediated currents contribute to fasting-induced activation of these neurons. Genetic mutation of SK3 specifically in AgRP/NPY neurons leads to increased sensitivity to diet-induced obesity, associated with chronic hyperphagia and decreased energy expenditure. Our results identify SK3 as a key intrinsic

*Correspondence: yongx@bcm.edu.

AUTHOR CONTRIBUTIONS

Y.H. and G.S. conducted most of experiments, collected and analyzed data, and wrote the manuscript. P.X. and Y. Xia assisted with the histology study. C.W., K.S., A.H., and X.Y. assisted with surgical procedures and the production of study mice. C.L., Q.W., and Q.T. were involved in study design and manuscript writing. Y. Xu is the guarantor of this work and, as such, had full access to all the data in the study and takes responsibility for the integrity of the data and the accuracy of the data analysis.

SUPPLEMENTAL INFORMATION

Supplemental Information includes Supplemental Experimental Procedures, six figures, and one table and can be found with this article online at http://dx.doi.org/10.1016/j.celrep.2016.10.044.

mediator that coordinates nutritional status with AgRP/NPY neural activities and animals' feeding behavior and energy metabolism.

Graphical Abstract

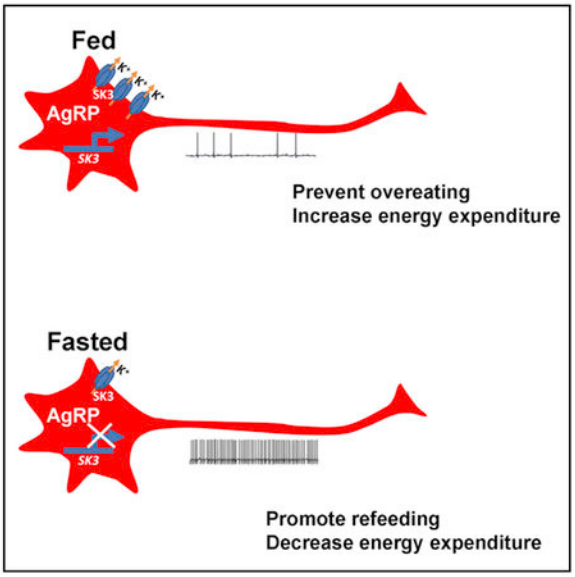

In Brief

Firing activities of AgRP/NPY neurons are essential for energy homeostasis. Heet al. demonstrate that SK3-mediated currents inhibit AgRP/NPY neurons in satiated mice and decreased SK3 expression contributes to fasting-induced activation of these neurons. Thus, dynamic SK3 functions coordinate nutritional status with AgRP/NPY neural activities and animals' energy balance.

INTRODUCTION

Normal feeding behavior is essential for survival and homeostatic control of energy balance. Increased feeding is associated with obesity, a major health issue in Western societies. Neurons that co-express agouti-related peptide (AgRP) and neuropeptide Y (NPY) in the arcuate nucleus of hypothalamus (ARH) are indispensable for normal feeding behavior. For example, genetic ablation of these AgRP/NPY neurons in adult mice leads to severe anorexia and death within a few days (Wu et al., 2009). On the other hand, selective activation of AgRP/NPY neurons rapidly promotes eating, even when mice are satiated (Aponte et al., 2011; Krashes et al., 2011).

Activities of AgRP/NPY neurons are tightly regulated by nutritional status. For example, AgRP/NPY neurons in satiated animals are more inhibited than those in fasted animals (Yang et al., 2011), which is essential to prevent overeating. Further, the availability of food cues, but not necessarily the consumption of food, rapidly suppresses firing of AgRP/NPY neurons (Betley et al., 2015; Chen et al., 2015; Mandelblat-Cerf et al., 2015), which may reflect a termination of the drive to find food. On the other hand, fasting remarkably

enhances AgRP/NPY neural activity (Yang et al., 2011), which promotes animals to eat and reserve energy. Thus, AgRP/NPY neural activities coordinate feeding behavior with food availability and are crucial for animals' survival. Emerging evidence started to reveal the mechanisms by which nutritional status regulates AgRP/NPY neural activities. It has been shown that during fasting, reduced leptin signaling results in large and persistent activation of AgRP/NPY neural activity (Takahashi and Cone, 2005). In parallel, elevated circulating ghrelin during fasting acts upon presynaptic terminals to trigger glutamate release, which in turn activates AgRP/NPY neurons (Yang et al., 2011). In satiated animals, insulin directly activates AgRP/NPY neurons via K_{ATP}-dependent mechanisms (Könner et al., 2007). Further, leptin acts through pro-opiomelanocortin (POMC) neurons, which release β-endorphin to inhibit the presynaptic glutamate release and therefore suppress AgRP/NPY neurons (Yang et al., 2011). Consistently, genetic deletion of glutamate NMDA receptors selectively in AgRP/NPY neurons attenuates their neural activities, and NMDA-mediated currents have been implicated to mediate fasting-induced synaptogenesis and spinogenesis in AgRP/NPY neurons (Liu et al., 2012) via AMP-kinase-dependent mechanisms (Kong et al., 2016). In addition to these well-defined external signals, intrinsic neural plasticity within AgRP/NPY neurons may also contribute to the dynamic firing activities of AgRP/NPY neurons at different nutritional states. However, these intrinsic mechanisms remain to be fully understood.

Small-conductance calcium-activated potassium (SK) channels are activated by elevations in cytosolic calcium from several different sources, including calcium influx via NMDA receptors (Faber et al., 2005; Ngo-Anh et al., 2005). The opening of SK channels allows potassium outflux, which is believed to constitute a large portion of the after-hyperpolarization (AHP) (Adelman et al., 2012). SK3 (encoded by the *Kcnn3* gene) is an SK isoform (Köhler et al., 1996) and is abundantly expressed in the ARH, while the levels of other isoforms (SK1, SK2, and SK4) in the ARH are minimal (Stocker and Pedarzani, 2000). A recent study demonstrated that SK3 mRNA levels in AgRP/NPY neurons undergo the most robust reduction after a 24-hr food deprivation and that pharmacological inhibition of SK currents can activate AgRP/NPY neurons (Henry et al., 2015). These raised a possibility that SK3-mediated potassium currents may contribute to the dynamic changes in AgRP/NPY neural activity during the fed-to-fasted transition.

Here, we first used immunofluorescent staining to confirm that SK3 proteins in AgRP/NPY neurons undergo dramatic reductions after food deprivation. We further combined pharmacology and a genetic mouse model with electrophysiology to establish that SK3-mediated currents contribute to the dynamic changes in AgRP/NPY neural activity during the fed-to-fasted transition. Finally, we systematically analyzed the metabolic phenotypes of mice lacking SK3 only in AgRP/NPY neurons and demonstrated that loss of SK3 function in AgRP/NPY neurons impairs normal regulation of feeding behavior and energy balance in mice.

RESULTS

Fasting Reduces SK3 Proteins and SK-Mediated Currents in AgRP/NPY Neurons

A 24-hr food deprivation robustly reduces mRNA levels of SK3 in AgRP/NPY neurons in mice, and a selective SK channel inhibitor, apamin, can stimulate firing of AgRP/NPY neurons (Henry et al., 2015). Here, we first used double immunofluorescence staining for SK3 and GFP in NPY-GFP mice (Pinto et al., 2004) to confirm that a 24-hr food deprivation exceptionally diminished SK3 protein levels in AgRP/NPY neurons (Figures S1A and S1B) and was associated with significant reductions in apamin-sensitive SK-mediated currents (Figures S1C–S1E). This fasting-induced SK3 reduction appears to be specific to AgRP/NPY neurons, as SK3 expression in the paraventricular nucleus of the hypothalamus was not changed by food deprivation (Figure S2).

Pharmacological Inhibition of SK Channels Activates AgRP/NPY Neurons

SK currents are known to constitute the AHP of an action potential (Adelman et al., 2012). Thus, we further analyzed the AHP of AgRP/NPY neurons during fed and fasted conditions, in the absence or presence of apamin. First, we found that AgRP/NPY neurons from fed mice displayed a significantly larger AHP than those from fasted mice (Figures S3A and S3B). Importantly, a chronic incubation of apamin (100 nM, 2 hr) normalized the AHP in AgRP/NPY neurons from fed mice to the level of untreated AgRP/NPY neurons from fasted mice (Figures S3A and S3B). The AHP influences the voltage trajectory between action potentials, and ultimately affects the intrinsic excitability of neurons (Madison and Nicoll, 1982). Indeed, activation of SK currents decreases excitability and firing rate in various types of neurons (Chen and Toney, 2009; Maher and Westbrook, 2005; Mateos-Aparicio et al., 2014). Thus, we further examined the firing activities of AgRP/NPY neurons. We observed that the firing rate of untreated AgRP/NPY neurons was significantly lower in the fed condition than in the fasted condition (Figures S3C and S3D). These findings are consistent with previous reports (Liu et al., 2012; Takahashi and Cone, 2005; Yang et al., 2011) and indicate that feeding inhibits the firing activity of AgRP/NPY neurons. Interestingly, incubation with apamin (100 nM, 2 hr) significantly increased the firing rate of fed AgRP/NPY neurons to the level of untreated fasted neurons (Figures S3C and S3D). Notably, the resting membrane potential was not changed in these conditions (Figures S3C and S3E). Similar effects of apamin have been reported previously (Henry et al., 2015). Collectively, these results indicate that endogenous SK currents are required to constitute AHP and inhibit AgRP/NPY neural activity in the fed condition.

Genetic Mutation of SK3 Channels Activates AgRP/NPY Neurons

In order to examine the physiological roles of SK3 in AgRP/NPY neurons, we generated a mutant mouse model ($Kcnn3^{f/f}$/AgRP-CreERT2). Injections of tamoxifen in these mice induced Cre recombinase activity specifically in mature AgRP/NPY neurons, and therefore resulted in recombination of floxed Kcnn3 allele in these neurons (named AgRP-SK3-KO). Here, we confirmed that the recombined floxed Kcnn3 allele was only detected in the AgRP-containing ARH region in AgRP-SK3-KO mice (Figure 1A). We detected apamin-sensitive SK-mediated currents in fed AgRP/NPY neurons from control mice that were significantly reduced by food deprivation (Figures 1B and 1C). Importantly, the SK-mediated currents

were significantly reduced in AgRP/NPY neurons from AgRP-SK3-KO mice, regardless of whether these mice were satiated or food deprived (Figures 1B and 1C), confirming the loss of SK3 function in AgRP/NPY neurons. However, using the same SK3 antibody, we still detected weak immunoreactivity in AgRP/NPY neurons (Figure S4). Thus, we suggest that the recombination on the floxed Kcnn3 allele resulted in a mutant SK3 protein rather than a total loss of the protein. While this mutant protein clearly loses its ability to mediate potassium currents (as shown in Figures 1B and 1C), the SK3 antibody we used could not fully distinguish the mutant protein from wild-type SK3 protein.

Further, we showed that in control mice, the AHP in AgRP/NPY neurons was significantly reduced by food deprivation (Figures 1D and 1E). Importantly, the AHP in AgRP/NPY neurons from fed AgRP-SK3-KO mice was significantly smaller than that from fed control mice; food deprivation did not further reduce the AHP in these neurons from AgRP-SK3-KO mice (Figures 1D and 1E). Similarly, the firing rate in AgRP/NPY neurons in control mice was significantly increased by food deprivation; the firing rate in AgRP/NPY neurons from fed AgRP-SK3-KO mice was significantly increased compared to that from fed control mice, and food deprivation did not further increase the firing rate in these neurons from AgRP-SK3-KO mice (Figures 1F and 1G). Notably, the resting membrane potential was not altered (Figures 1F and 1H). In summary, genetic mutation of SK3 in AgRP/NPY neurons reduced SK-mediated currents and AHP and increased firing rate. Notably, all of these phenotypes resulting from SK3 mutation were similar, but not additive, to the effects caused by food deprivation.

It has been shown that excitatory inputs to AgRP/NPY neurons are significantly higher at the onset of the dark cycle than in the early light cycle (Yang et al., 2011), and the neural activity of these neurons is significantly higher during the dark cycle than the light cycle (Krashes et al., 2013). Thus, we compared electro-physiological properties of AgRP/NPY neurons at 9 a.m. versus 5:30 p.m. (30 min prior to the dark cycle) in control and AgRPSK3-KO mice. We observed that in control mice, SK-mediated currents were significantly lower at 5:30 p.m. than at 9 a.m. (Figure 2A), and this was associated with decreased AHP (Figure 2B) and increased firing rate at 5:30 p.m. (Figure 2C) compared to 9 a.m. In AgRP-SK3-KO mice, at both time points, SK-mediated currents were very low (Figure 2A), which was associated with constant low AHP and high firing rate (Figures 2B and 2C). The resting membrane potential was not altered among these groups (Figure 2D). These results indicate that SK3-mediated currents contribute to the dynamic changes in AgRP/NPY neural activities at the light-to-dark-cycle transition.

SK channels can be activated by calcium influx through NMDA receptors (Faber et al., 2005; Ngo-Anh et al., 2005), and inhibition of SK currents has been shown to potentiate NMDA currents in dopamine neurons (Soden et al., 2013) and amygdala neurons (Faber et al., 2005). Here, we found that NMDA-induced currents were significantly potentiated in AgRP/NPY neurons from fasted control mice compared to those from fed control mice (Figures 3A and 3B). Importantly, AgRP/NPY neurons from fed AgRPSK3-KO mice exhibited significantly larger NMDA-induced currents than those from fed control mice, and food deprivation did not further increase NMDA-induced currents in AgRP/NPY neurons from AgRP-SK3-KO mice (Figures 3A and 3B). In addition, using a current-clamp protocol,

we showed that NMDA depolarized AgRP/NPY neurons and increased their firing rate at the fed condition; importantly, these NMDA-induced responses were significantly enhanced in fed AgRP-SK3-KO mice compared to fed control mice (Figures 3C–3E). Collectively, these data indicate that high SK3-mediated currents at the fed condition reduce NMDA-induced currents in AgRP/NPY neurons while low SK3-mediated currents at the fasted condition function to amply NMDA-induced currents and therefore AgRP/NPY neural activation.

We also compared electrophysiological properties of AgRP/NPY neurons in control and AgRP-SK3-KO mice fed with chow or a high-fat diet (HFD) for 4 weeks. Regardless of whether fed with chow or HFD, AgRP/NPY neurons from AgRP-SK3-KO mice showed significantly reduced SK-mediated currents compared to control mice (Figure S5A), as well as significant increases in NMDA-induced currents (Figure S5B) and firing rate (Figure S5C) but no changes in the resting membrane potentials (Figure S5D). However, HFD feeding failed to alter these parameters in either control or AgRP-SK3-KO mice (Figures S5A–S5D).

Loss of SK3 Channels in AgRP/NPY Neurons Leads to Hyperphagia and Obesity in HFD-Fed Mice

To further examine the physiological roles of SK3 in AgRP/NPY neurons in the regulation of food intake and body weight balance, we first characterized the long-term metabolic phenotypes of AgRP-SK3-KO mice with chronic ad libitum chow-feeding. Shortly after tamoxifen injections to induce SK3 mutation, chow-fed AgRP-SK3-KO mice showed modest but significant increases in body weight compared to chow-fed control mice (Figure S6A). However, this body weight difference dissipated ~2 weeks later, and the two groups had comparable body weights throughout the rest of chow-feeding period (Figure S6A). Given that there was a small difference in body weight prior to tamoxifen induction, we also calculated the changes in body weight since tamoxifen induction but found no significant differences between groups (Figure S6B). Surprisingly, despite the lack of differences in body weight, chow-fed AgRP-SK3-KO mice showed subtle but significant increases in chow intake (Figure S6C). We then surgically implanted telemetric Mini Mitter probes (Xu et al., 2015) into the abdominal cavity to monitor body temperature and physical activity in a separate cohort of mice. We found that chow-fed AgRP-SK3-KO mice showed significantly increased body temperature and physical activity compared to their control littermates at multiple time points during the dark cycle (Figures S6D and S6E), which may account for the lack of differences in body weight despite hyperphagia.

We then fed another cohort of male AgRP-SK3-KO and control littermates an HFD ad libitum. HFD-fed AgRP-SK3-KO male mice showed significant increases in body weight gain and HFD intake compared to HFD-fed control males (Figures 4A and 4B). The body weight gain was associated with a significant increase in fat mass and a trended increase in lean mass (Figure 4C). Consistently, weights of gonadal white adipose tissue (gWAT) and interscapular brown adipose tissue (BAT) were significantly higher in AgRP-SK3-KO male mice than in control mice, although the weight of inguinal adipose tissue (iWAT) was comparable between the two groups (Figures 4D–4F). Interestingly, we also found that

mRNA levels of multiple BAT genes, including UCP1, PGC1α, and PRDM16, were significantly lower in AgRP-SK3-KO mice than in control mice (Figure 4G).

Abnormal Feeding Behaviors in Mice with Mutant SK3 in AgRP/NPY Neurons

To further determine the role of SK3 channels in AgRP/NPY neurons in the regulation of feeding behavior, we adapted a cohort of body-weight-matched HFD-fed AgRP-SK3-KO male mice and their control littermates into BioDaq chambers to monitor their feeding behavior. During a 24-hr period with ad libitum feeding, AgRP-SK3-KO mice consumed significantly more food than control mice (Figure 5A). This hyperphagia was associated with significant increases in meal size (Figure 5B), while meal frequency was not altered (Figure 5C). We then subjected these mice to a 24-hr fast followed by a 24-hr refeeding. Surprisingly, during the refeeding period, AgRP-SK3-KO mice consumed significantly less food than control mice (Figure 5A). We then assessed effects of the 24-hr food deprivation on food intake, meal size, and meal frequency within the same group. In control mice, food deprivation evoked the expected increases in food intake during the refeed period and was associated with increased meal size and unchanged meal frequency (Figures 5A–5C, white bars). On the other hand, food deprivation failed to produce increases in food intake and meal size during the re-feed period in AgRP-SK3-KO mice, although these mice exhibited a slight increase in meal frequency (Figures 5A–5C, black bars). Thus, ad libitum AgRP-SK3-KO mice showed an increase in food intake and meal size but failed to enhance refeeding after 24-hr food deprivation.

Abnormal Energy Metabolism in Mice with Mutant SK3 in AgRP/NPY Neurons

To further determine the role of SK3 channels in AgRP/NPY neurons in the regulation of energy metabolism, we adapted another cohort of body-weight-matched HFD-fed AgRP-SK3-KO male mice and their control littermates into Comprehensive Lab Animal Monitoring System (CLAMS) metabolic chambers and subjected these mice to a 3-day ad libitum to fast to refeed paradigm. Compared to control mice, AgRP-SK3-KO male mice showed significantly lower energy expenditure at multiple time points during the ad libitum and refeed periods; such decreased energy expenditure was observed at fewer time points during the fast period (Figure 6A). Consistently, the daily energy expenditure was significantly lower in AgRP-SK3-KO male mice than in control mice both at the ad libitum and refeed periods, but no difference was observed during the fast period (Figure 6B). As expected, both AgRP-SK3-KO mice and their controls responded to food deprivation with significant reductions in energy expenditure; during the refeed period, energy expenditure was normalized to the level measured during the ad libitum period (Figure 6B).

The respiratory exchange rate (RER) was slightly higher in AgRP-SK3-KO mice than in control mice at a few time points during the ad libitum period (Figure 6C), although the daily average RER during the ad libitum period was not significantly different between groups (Figure 6D). No difference in RER was observed between the two genotypes during the fast period. Interestingly, the RER was significantly lower in AgRP-SK3-KO mice than in control mice at a few time points during the refeed period (Figure 6C), although the daily average RER during this period was not significantly different between groups (Figure 6D). We also analyzed effects of fasting and refeeding on the RER in each group of mice.

Notably, control mice showed significantly decreased RER during the fast period compared to the ad libitum period, indicating increased fat oxidation during food deprivation; during the refeed period, RER rebounded and overshot to a level that was significantly higher than that measured during the ad libitum period (Figure 6D, white bars). Interestingly, the RER in AgRP-SK3-KO mice did not show this overshoot during the refeed period, although a similar reduction was observed during the fast period (Figure 6D, black bars).

We also analyzed the physical activity (ambulation and rearing activity) of these mice in CLAMS metabolic chambers. Compared to control mice, AgRP-SK3-KO mice showed decreases in ambulation or rearing activities at some time points but increases at other time points (Figures 6E and 6G). Overall, there were no significant differences in daily ambulation or rearing activities (Figures 6F and 6H).

DISCUSSION

Food deprivation remarkably enhances AgRP/NPY neural activity (Liu et al., 2012; Takahashi and Cone, 2005; Yang et al., 2011). Increased AgRP/NPY neural activity increases food intake (Aponte et al., 2011; Krashes et al., 2011) and promotes animals to forage for food despite potential dangers (Padilla et al., 2016). Activation of AgRP/NPY neurons also inhibits anxiety (Dietrich et al., 2015) and aggression (Padilla et al., 2016), which facilitate food seeking and feeding. In addition, activation of AgRP/NPY neurons suppresses energy expenditure to reserve energy (Krashes et al., 2013; Ruan et al., 2014). Thus, increased AgRP/NPY neural activity during food deprivation is believed to be an essential adaptive mechanism that coordinates complex behaviors and energy metabolism in order to ensure survival, yet how AgRP/NPY neural activity is elevated by fasting remains to be fully understood.

Here, we provide evidence that dynamic expression levels of SK3 channels in AgRP/NPY neurons mediates the dynamic firing activities of these neurons during the fed-to-fasted transition. First, we observed that the majority of AgRP/NPY neurons from satiated mice express high levels of SK3 proteins, whereas a 24-hr food deprivation exceptionally diminishes SK3 protein levels in these neurons. These dynamic changes in SK3 protein levels are consistent with a recent RNA sequencing (RNA-seq) study demonstrating that SK3 mRNAs in AgRP/NPY neurons undergo a 5.4-fold reduction after food deprivation (Henry et al., 2015). Given the consistent changes at the levels of proteins and mRNAs, we suggest that SK3 transcription is suppressed during fasting, which results in decreased levels of SK3 proteins, although the transcription factor or factors responsible for this regulation remain unclear. Consistent with decreased SK3 protein levels, we observed that SK-mediated potassium currents were significantly reduced in AgRP/NPY neurons from fasted mice compared to those from fed mice. Further, at the functional level, we showed that apamin (a pharmacological inhibitor of SK currents) robustly activated AgRP/NPY neurons from fed mice, as demonstrated by reduced AHP and elevated firing rate. Notably, apamin treatment brought these parameters from the fed condition to a level similar to the fasted condition. These observations with apamin treatment were consistent with an earlier report (Henry et al., 2015) and argue that endogenous SK-mediated currents contribute to the inhibition of AgRP/NPY neurons in the satiated state.

However, because apamin may inhibit all isoforms of SK channels, these pharmacological results could not fully establish the functional relevance of SK3 in AgRP/NPY neurons. To tackle this issue, we generated and validated a mouse model with SK3 genetically mutated in AgRP/NPY neurons. Using this mouse model, we showed that loss of SK3 function from AgRP/NPY neurons resulted in activation of these neurons in the fed condition to a level similar to the fasted condition in control mice. Importantly, food deprivation in the mutant mice did not further activate AgRP/NPY neurons. Given that the activation of AgRP/NPY neurons caused by SK3 mutation was not additive with that evoked by food deprivation, we believe that fasting-induced AgRP/NPY neural activation is largely mediated by the reduction in endogenous SK3 levels.

Notably, elevated glutamate release onto AgRP/NPY neurons has been implicated in the enhanced AgRP/NPY neural activities in fasted state (Yang et al., 2011). Further, genetic deletion of glutamate NMDA receptors selectively in AgRP/NPY neurons blunts the fasting-induced activation of these neurons as well as synaptogenesis and spinogenesis (Liu et al., 2012). SK channels are known to be activated by calcium influx through NMDA receptors, and SK-mediated currents then reduce the amplitude of NMDA-induced calcium transients to form a negative feedback loop (Faber et al., 2005; Ngo-Anh et al., 2005). Here, we showed that food deprivation enhanced the amplitude of NMDA-induced currents in AgRP/NPY neurons from control mice. Importantly, loss of SK3 function resulted in a similar potentiation of NMDA-induced currents, and food deprivation in the mutant mice failed to further enhance NMDA-induced currents. Thus, we suggest that SK3 channels may function as an important “gate” to fine-tune NMDA-induced currents and therefore regulate dynamic firing of AgRP/NPY neurons at the fed-to-fasted transition. In particular, when animals are satiated, AgRP/NPY neurons express high levels of SK3, and SK3-mediated potassium currents suppress NMDA-induced inward currents, which results in an overall inhibition of AgRP/NPY neural activity; on the other hand, when animals are deprived with nutrients, SK3 expression is dramatically suppressed in AgRP/NPY neurons, which allows amplification of NMDA-induced currents and therefore activation of AgRP/NPY firing.

Certainly, SK3 is not the only mediator for the dynamic changes in AgRP/NPY firing activities. It is worth noting that the wide range of firing rates in AgRP/NPY neurons from control mice partly overlaps with that seen in AgRP-SK3-KO mice, although these two groups are statistically different from each other. The variable firing rates of AgRP/NPY neurons within the same group likely reflect the fact that AgRP/NPY neurons are different from each other in that they express different sets of ion channels (not just SK3 but many others), receptors, and signaling molecules (Henry et al., 2015), which in combination constitute the absolute firing rate for each AgRP/NPY neuron. For example, a delayed rectifier Kv channel (Kv7.3) can be modified by O-GlcNAc transferase (OGT) after food deprivation (Ruan et al., 2014). Interestingly, selective deletion of OGT in AgRP/NPY neurons results in decreased firing of these neurons and leads to enhanced energy expenditure (Ruan et al., 2014). In addition, a voltage-gated sodium channel (Nav1.7) in AgRP/NPY neurons has recently been shown to prolong the duration of excitatory postsynaptic potentials and maintain synaptic integration; loss of Nav1.7 in AgRP/NPY neurons resulted in decreased in body weight (Branco et al., 2016).

We observed that ad libitum AgRP-SK3-KO mutant mice are hyperphagic regardless of whether they are fed with regular chow or an HFD. We attributed this chronic hyperphagia to the high firing activity of AgRP/NPY neurons that we observed in these mutant mice. Supporting this, chemogenetic activation of AgRP/NPY neurons has been shown to trigger sustained increases in food intake for up to 24 hr (Krashes et al., 2013). Detailed analyses on meal patterns further revealed that these mutant mice had increased meal size but normal meal frequency. These results indicate that SK3 in AgRP/NPY neurons is required to mediate normal satiety signals to prevent ad libitum animals from overeating. Thus, our results support a model where the levels of SK3 in AgRP/NPY neurons are regulated by nutritional status, and these dynamic SK3 levels and SK3-mediated potassium currents contribute to the changes in AgRP/NPY neural activities and ultimately coordinate appropriate feeding behavior in response to different nutritional states.

Despite the chronic hyperphagia, chow-fed AgRP-SK3-KO mice showed comparable body weight as control mice. Notably, chow-fed mutant mice showed modest increases in body temperature and physical activity, which may reflect a compensatory response to dissipate excess energy. On the other hand, HFD-fed AgRP-SK3-KO mice showed increased body weight gain, which was associated with hyperphagia and hyperadiposity. These obese phenotypes should be attributed at least partly to increased HFD intake. Interestingly, we also observed reduced energy expenditure in HFD-fed AgRP-SK3-KO mice, which should partly contribute to obesity development in these mice. It is worth noting that decreased energy expenditure was only observed when AgRP-SK3-KO mice were fed ad libitum or refed and was not seen in the mutant mice that were fasted. This pattern is consistent with our electrophysiological observations that loss of SK3 function increased the firing of AgRP/NPY neurons in the fed condition but did not affect firing in the fasted condition. The lack of phenotypes in fasted mice is conceivable, because control mice also lose SK3 proteins and SK-mediated currents in AgRP/NPY neurons during food deprivation, which mimics genetic mutation of SK3 in the mutant mice. The decreased energy expenditure during the refeed period could be attributed partly to the decreased food intake observed in AgRP-SK3-KO mice. However, during the ad libitum period, when these mutant mice ate more, AgRP-SK3-KO mice showed a similar reduction in energy expenditure. Thus, this decreased energy expenditure is likely a direct outcome of SK3 mutation in AgRP/NPY neurons. Notably, the reductions in energy expenditure were associated with decreases in thermogenic gene expression in BAT (including UCP1), suggesting that decreased thermogenesis may contribute to the decreased overall energy expenditure. These results are consistent with the known effect of AgRP/NPY neurons on the suppression of energy expenditure (Krashes et al., 2011) and highlight an important role of SK3 in AgRP/NPY neurons in the regulation of energy expenditure.

A series of coordinated behavioral and metabolic responses are necessary for animals to survive food deprivation. These responses include suppression of energy expenditure during fasting, but animals also need to engage in enhanced refeeding to quickly restore energy balance when food becomes available again. In support of this, we found that control mice ate significantly more food during the 24-hr refeed period than the ad libitum period. On the other hand, during the refeeding period, AgRP-SK3-KO mice ate as much food as they did prior to the fast. Importantly, the amount of refeed was significantly lower in mutant mice

than in control mice. In other words, the loss of SK3 in AgRP/NPY neurons, while resulting in a constant higher ad libitum food intake, reduces the dynamic range of feeding. Such findings are quite surprising given the comparable firing activities of AgRP/NPY neurons between fasted control and fasted AgRP-SK3-KO mice. We speculate that activities of other neural circuits, such as GABAergic neurons in the lateral hypothalamus (Jennings et al., 2015; Wu et al., 2015) and in the bed nucleus of stria terminalis (Jennings et al., 2013), may also contribute to the full exhibition of fast-induced refeeding; however, functions of these circuits may have been disrupted due to elevated firing of AgRP/NPY neurons in mutant mice.

Notably, we also observed that control mice showed a “rebound” in the RER during the refeed period, which was significantly higher than the baseline RER during the ad libitum condition. We speculate that this enhanced RER may be secondary to enhanced food intake. Nevertheless, an elevated RER indicates decreased fat oxidation during the refeed period and may represent an important metabolic adaptation for animals to rebuild fat storage, which has been damaged during food deprivation. Interestingly, AgRP-SK3-KO mice did not show such a rebound in the RER, although RER during the re-feed period recovered to the same baseline level during the ad libitum. Given that AgRP/NPY neurons have been implicated in the control of peripheral substrate utilization and nutrient partitioning (Joly-Amado et al., 2012), we suggest that the loss of RER rebound may result directly from the loss of SK3 in AgRP/NPY neurons. Of course, we could not rule out the possibility that such RER phenotypes were secondary to the unaltered food intake during the refeed period versus the ad libitum period.

In summary, our results indicate that food deprivation reduces SK3-mediated currents in AgRP/NPY neurons and enhances their firing rate. On the other hand, feeding inhibits the firing of AgRP/NPY neurons, which is accompanied by robust SK3-mediated currents. Importantly, inhibition of SK currents by a pharmacological blocker (apamin) or by genetic mutation of SK3 resulted in robust increases in the firing activity of fed AgRP/NPY neurons, partly through amplified NMDA-induced currents. Together, these findings support a model in which SK3-mediated currents primarily function during satiation to inhibit AgRP/NPY neural activity; on the other hand, food deprivation decreases SK3 expression and therefore suppresses SK currents, which contributes to the increased excitability of AgRP/NPY neurons during fasting. The loss of SK3 in AgRP/NPY neurons not only renders ad libitum mice more susceptible to hyperphagia and diet-induced obesity but also impairs the flexibility of feeding, especially after food deprivation.

EXPERIMENTAL PROCEDURES

Mice

For electrophysiological studies, we crossed the Rosa26-tdTOMATO allele onto regular AgRP-Cre mice (Tong et al., 2008) to generate AgRP-Cre/Rosa26-tdTOMATO mice, which express TOMATO selectively in AgRP/NPY neurons. We also crossed C57Bl6 mice (purchased from the mouse facility of Baylor College of Medicine) with NPY-GFP mice (Pinto et al., 2004) to generate NPY-GFP mice. These mice were used to examine colocalization of SK3 with AgRP/NPY neurons.

In order to generate mice lacking SK3 specifically in AgRP/NPY neurons, we first crossed $Kcnn3^{f/f}$ mice (Deignan et al., 2012) (Jackson Laboratory, #019083) to AgRP-Cre mice (Tong et al., 2008) (also known as AgRP-IRES-Cre, Jackson Laboratory, #012899) to generate $Kcnn3^{f/f}$/AgRP-Cre mice. However, many of these $Kcnn3^{f/f}$/AgRP-Cre mice showed mosaic deletion as demonstrated by a recombined Kccn3 allele in tail DNA, and we were not able to generate any cohorts. Thus, we took an alternative strategy, crossing $Kcnn3^{f/f}$ mice with recently generated tamoxifen-inducible AgRP-CreERT2 mice (Wang et al., 2013), to generate $Kcnn3^{f/f}$/AgRP-CreERT2 (AgRP-SK3-KO) and their control littermates ($Kcnn3^{f/+}$/AgRP-CreERT2 and $kcnn3^{+/+}$/AgRP-CreERT2). At 7 weeks of age, both strains of mice received five tamoxifen injections (4 mg per injection), and the first two injections were coupled with 24-hr food deprivation (separated by 48 hr) to enhance Agrp promoter activity. These AgRP-SK3-KO and their control littermates were used for the feeding study and metabolic characterization (Figures 4, 5, and 6). In some breedings, we also introduced the Rosa26-tdTOMATO allele onto AgRP-CreERT2 and $Kcnn3^{f/f}$/AgRP-CreERT2 mice, respectively. These crosses generated control and AgRPSK3-KO mice with TOMATO selectively expressed in AgRP/NPY neurons (after tamoxifen inductions). These mice were used for electrophysiological studies.

All the breeders were backcrossed to the C57Bl6 background for more than 12 generations. Mice were housed in a temperature-controlled environment in groups of two to five at 22°C–24°C using a 12 hr light/12 hr dark cycle. All mice were fed on standard chow (6.5% fat, #2920, Harlan-Teklad) ad libitum, unless mentioned otherwise. Water was provided ad libitum.

Electrophysiology

Mice were either fed ad libitum or fasted for 24 hr before the experiments. At 9:00 a.m. to 9:30 a.m. (unless mentioned otherwise), these mice were deeply anesthetized with isoflurane and transcardially perfused (Hill et al., 2008) with a modified ice-cold artificial cerebral spinal fluid (aCSF; containing 10 mM NaCl, 25 mM $NaHCO_3$, 195 mM sucrose, 5 mM glucose, 2.5 mM KCl, 1.25 mM NaH_2PO_4, 2 mM Na pyruvate, 0.5 mM $CaCl_2$, and 7 mM $MgCl_2$) (Ren et al., 2012). The mice were then decapitated, and the entire brain was removed. Brains was quickly sectioned in ice-cold aCSF solution (containing 126 mM NaCl, 2.5 mM KCl, 1.2 mM $MgCl_2$, 2.4 mM $CaCl_2$, 1 mM NaH_2PO_4, 11.1 mM glucose, and 21.4 mM $NaHCO_3$) (Pinto et al., 2004) saturated with 95% O_2 and 5% CO_2. Coronal sections containing the ARH (250 μm) were cut with a Microm HM 650V vibratome (Thermo Fisher Scientific). The slices were then recovered in aCSF (Pinto et al., 2004) at 34°C for 1 hr.

Whole-cell patch-clamp recordings were performed in the TOMATO-labeled AgRP/NPY neurons in the ARH visually identified by an upright microscope (Eclipse FN-1, Nikon) equipped with IR-DIC optics (Nikon 40× NIR). Signals were processed using a Multiclamp 700B amplifier (Axon Instruments), sampled using Digidata 1440A, and analyzed offline on a PC with pCLAMP 10.3 (Axon Instruments). The slices were bathed in oxygenated aCSF (Pinto et al., 2004) (32°C–34°C) at a flow rate of ~2 mL/min. Patch pipettes with resistances of 3–5 MΩ were filled with solution containing 126 mM K gluconate, 10 mM NaCl, 10 mM EGTA, 1 mM $MgCl_2$, 2 mM Na-ATP, and 0.1 mM Mg-GTP (adjusted to pH 7.3 with KOH)

(Pagadala et al., 2013). A voltage-clamp protocol was used to record SK-mediated currents, as performed previously (Cao et al., 2014). Acute perfusion with apamin (100 nM for 6 min) was used to confirm a blockade of the SK-mediated currents with this selective SK channel inhibitor (Pagadala et al., 2013). We also used a gap-free model to record the current induced by NMDA (500 μm, puff 1 s) in AgRP/NPY neurons by holding the potential at [C0]60 mV (Wirkner et al., 2007). Current clamp was engaged to test the firing rate and AHP of action potentials, as well as the resting membrane potential. For some experiments, chronic apamin incubation (100 nM, 2 hr) (Pagadala et al., 2013) was used to test the effects of SK channel inhibition on these parameters. At the end of recordings, lucifer yellow dye was included in the pipette solution to trace the recorded neurons, and the brain slices were fixed with 4% formalin overnight and mounted onto slides. Cells were then visualized with the Leica DM5500 fluorescence microscope to identify post hoc the anatomical location of the recorded neurons in the ARH.

BioDaq Feeding Study

A cohort of male control and AgRP-SK3-KO littermates were fed with an HFD (65% fat, #D12492, Research Diets) and acclimated to the BioDaq feeding chambers (Research Diets) for 7 days. These body-weight-matched mice were then subjected to a 3-day feeding paradigm in which they were fed ad libitum during the first 24 hr (6:00 p.m. to 6:00 p.m.), food deprived during the second 24-hr period (6:00 p.m. to 6:00 p.m.), and refed for the last 24-hr period (6:00 p.m. to 6:00 p.m.). Food intake was monitored for the entire 3-day period. Meals were defined as food intake events with a minimum duration of 60 s and a break of 300 s between food-intake events.

Statistics

The minimal sample size was predetermined by the nature of the experiments. For most physiological readouts (e.g., food intake), at least six mice per group were included. For histology studies, four mice were included in each group. For electrophysiological studies, 10–40 neurons in each genotype or condition were included. The data are presented as mean ± SEM. Statistical analyses were performed using GraphPad Prism to evaluate normal distribution and variations within and among groups. Methods of statistical analyses were chosen based on the design of each experiment and are indicated in figure legends. $p < 0.05$ was considered to be statistically significant.

Study Approval

Care of all animals and procedures were approved by the Baylor College of Medicine Institutional Animal Care and Use Committee.

Supplementary Material

Refer to Web version on PubMed Central for supplementary material.

ACKNOWLEDGMENTS

This work was supported by grants from the NIH (R01DK093587 and R01DK101379 to Y. Xu.; R01DK092605 to Q.T.) and the American Diabetes Association (7–13-JF-61 to Q.W. and 1–15-BS-184 to Q.T.) and by postdoctoral

fellowships from the American Heart Association (13POST13800000 and 15POST22670017 to P.X.) and the Davis Foundation (C.L.).

REFERENCES

Adelman JP, Maylie J, and Sah P (2012). Small-conductance Ca2+-activated K+ channels: form and function. Annu. Rev. Physiol 74, 245–269. [PubMed: 21942705]

Aponte Y, Atasoy D, and Sternson SM (2011). AGRP neurons are sufficient to orchestrate feeding behavior rapidly and without training. Nat. Neurosci 14, 351–355. [PubMed: 21209617]

Betley JN, Xu S, Cao ZF, Gong R, Magnus CJ, Yu Y, and Sternson SM (2015). Neurons for hunger and thirst transmit a negative-valence teaching signal. Nature 521, 180–185. [PubMed: 25915020]

Branco T, Tozer A, Magnus CJ, Sugino K, Tanaka S, Lee AK, Wood JN, and Sternson SM (2016). Near-Perfect Synaptic Integration by Nav1.7 in Hypothalamic Neurons Regulates Body Weight. Cell 165, 1749–1761. [PubMed: 27315482]

Cao X, Xu P, Oyola MG, Xia Y, Yan X, Saito K, Zou F, Wang C, Yang Y, Hinton A, Jr., et al. (2014). Estrogens stimulate serotonin neurons to inhibit binge-like eating in mice. J. Clin. Invest 124, 4351–4362. [PubMed: 25157819]

Chen QH, and Toney GM (2009). Excitability of paraventricular nucleus neurones that project to the rostral ventrolateral medulla is regulated by small-conductance Ca2+-activated K+ channels. J. Physiol 587, 4235–4247. [PubMed: 19581379]

Chen Y, Lin YC, Kuo TW, and Knight ZA (2015). Sensory detection of food rapidly modulates arcuate feeding circuits. Cell 160, 829–841. [PubMed: 25703096]

Deignan J, Luján R, Bond C, Riegel A, Watanabe M, Williams JT, Maylie J, and Adelman JP (2012). SK2 and SK3 expression differentially affect firing frequency and precision in dopamine neurons. Neuroscience 217, 67–76. [PubMed: 22554781]

Dietrich MO, Zimmer MR, Bober J, and Horvath TL (2015). Hypothalamic Agrp neurons drive stereotypic behaviors beyond feeding. Cell 160, 1222–1232. [PubMed: 25748653]

Faber ES, Delaney AJ, and Sah P (2005). SK channels regulate excitatory synaptic transmission and plasticity in the lateral amygdala. Nat. Neurosci 8, 635–641. [PubMed: 15852010]

Henry FE, Sugino K, Tozer A, Branco T, and Sternson SM (2015). Cell type-specific transcriptomics of hypothalamic energy-sensing neuron responses to weight-loss. eLife 4, e09800.

Hill JW, Williams KW, Ye C, Luo J, Balthasar N, Coppari R, Cowley MA, Cantley LC, Lowell BB, and Elmquist JK (2008). Acute effects of leptin require PI3K signaling in hypothalamic proopiomelanocortin neurons in mice. J. Clin. Invest 118, 1796–1805. [PubMed: 18382766]

Jennings JH, Rizzi G, Stamatakis AM, Ung RL, and Stuber GD (2013). The inhibitory circuit architecture of the lateral hypothalamus orchestrates feeding. Science 341, 1517–1521. [PubMed: 24072922]

Jennings JH, Ung RL, Resendez SL, Stamatakis AM, Taylor JG, Huang J, Veleta K, Kantak PA, Aita M, Shilling-Scrivo K, et al. (2015). Visualizing hypothalamic network dynamics for appetitive and consummatory behaviors. Cell 160, 516–527. [PubMed: 25635459]

Joly-Amado A, Denis RG, Castel J, Lacombe A, Cansell C, Rouch C, Kassis N, Dairou J, Cani PD, Ventura-Clapier R, et al. (2012). Hypothalamic AgRP-neurons control peripheral substrate utilization and nutrient partitioning. EMBO J 31, 4276–4288. [PubMed: 22990237]

Köhler M, Hirschberg B, Bond CT, Kinzie JM, Marrion NV, Maylie J, and Adelman JP (1996). Small-conductance, calcium-activated potassium channels from mammalian brain. Science 273, 1709–1714. [PubMed: 8781233]

Kong D, Dagon Y, Campbell JN, Guo Y, Yang Z, Yi X, Aryal P, Well-enstein K, Kahn BB, Sabatini BL, and Lowell BB (2016). A postsynaptic AMPK→p21-activated kinase pathway drives fasting-induced synaptic plasticity in AgRP neurons. Neuron 91, 25–33. [PubMed: 27321921]

Könner AC, Janoschek R, Plum L, Jordan SD, Rother E, Ma X, Xu C, Enriori P, Hampel B, Barsh GS, et al. (2007). Insulin action in AgRP-expressing neurons is required for suppression of hepatic glucose production. Cell Metab 5, 438–449. [PubMed: 17550779]

Krashes MJ, Koda S, Ye C, Rogan SC, Adams AC, Cusher DS, Maratos-Flier E, Roth BL, and Lowell BB (2011). Rapid, reversible activation of AgRP neurons drives feeding behavior in mice. J. Clin. Invest 121, 1424–1428. [PubMed: 21364278]

Krashes MJ, Shah BP, Koda S, and Lowell BB (2013). Rapid versus delayed stimulation of feeding by the endogenously released AgRP neuron mediators GABA, NPY, and AgRP. Cell Metab. 18, 588–595. [PubMed: 24093681]

Liu T, Kong D, Shah BP, Ye C, Koda S, Saunders A, Ding JB, Yang Z, Sabatini BL, and Lowell BB (2012). Fasting activation of AgRP neurons requires NMDA receptors and involves spinogenesis and increased excitatory tone. Neuron 73, 511–522. [PubMed: 22325203]

Madison DV, and Nicoll RA (1982). Noradrenaline blocks accommodation of pyramidal cell discharge in the hippocampus. Nature 299, 636–638. [PubMed: 6289127]

Maher BJ, and Westbrook GL (2005). SK channel regulation of dendritic excitability and dendrodendritic inhibition in the olfactory bulb. J. Neurophysiol 94, 3743–3750. [PubMed: 16107526]

Mandelblat-Cerf Y, Ramesh RN, Burgess CR, Patella P, Yang Z, Lowell BB, and Andermann ML (2015). Arcuate hypothalamic AgRP and putative POMC neurons show opposite changes in spiking across multiple timescales. eLife 4, e07122.

Mateos-Aparicio P, Murphy R, and Storm JF (2014). Complementary functions of SK and Kv7/M potassium channels in excitability control and synaptic integration in rat hippocampal dentate granule cells. J. Physiol 592, 669–693. [PubMed: 24366266]

Ngo-Anh TJ, Bloodgood BL, Lin M, Sabatini BL, Maylie J, and Adelman JP (2005). SK channels and NMDA receptors form a Ca2+-mediated feedback loop in dendritic spines. Nat. Neurosci 8, 642–649. [PubMed: 15852011]

Padilla SL, Qiu J, Soden ME, Sanz E, Nestor CC, Barker FD, Quintana A, Zweifel LS, Rønnekleiv OK, Kelly MJ, and Palmiter RD (2016). Agouti-related peptide neural circuits mediate adaptive behaviors in the starved state. Nat. Neurosci 19, 734–741. [PubMed: 27019015]

Pagadala P, Park CK, Bang S, Xu ZZ, Xie RG, Liu T, Han BX, Tracey WD, Jr., Wang F, and Ji RR (2013). Loss of NR1 subunit of NMDARs in primary sensory neurons leads to hyperexcitability and pain hyper-sensitivity: involvement of Ca(2+)-activated small conductance potassium channels. J. Neurosci 33, 13425–13430. [PubMed: 23946399]

Pinto S, Roseberry AG, Liu H, Diano S, Shanabrough M, Cai X, Friedman JM, and Horvath TL (2004). Rapid rewiring of arcuate nucleus feeding circuits by leptin. Science 304, 110–115. [PubMed: 15064421]

Ren H, Orozco IJ, Su Y, Suyama S, Gutiérrez-Juárez R, Horvath TL, Wardlaw SL, Plum L, Arancio O, and Accili D (2012). FoxO1 target Gpr17 activates AgRP neurons to regulate food intake. Cell 149, 1314–1326. [PubMed: 22682251]

Ruan HB, Dietrich MO, Liu ZW, Zimmer MR, Li MD, Singh JP, Zhang K, Yin R, Wu J, Horvath TL, and Yang X (2014). O-GlcNAc transferase enables AgRP neurons to suppress browning of white fat. Cell 159, 306–317. [PubMed: 25303527]

Soden ME, Jones GL, Sanford CA, Chung AS, Güler AD, Chavkin C, Luján R, and Zweifel LS (2013). Disruption of dopamine neuron activity pattern regulation through selective expression of a human KCNN3 mutation. Neuron 80, 997–1009. [PubMed: 24206670]

Stocker M, and Pedarzani P (2000). Differential distribution of three Ca(2+)-activated K(+) channel subunits, SK1, SK2, and SK3, in the adult rat central nervous system. Mol. Cell. Neurosci 15, 476–493. [PubMed: 10833304]

Takahashi KA, and Cone RD (2005). Fasting induces a large, leptin-dependent increase in the intrinsic action potential frequency of orexigenic arcuate nucleus neuropeptide Y/Agouti-related protein neurons. Endocrinology 146, 1043–1047. [PubMed: 15591135]

Tong Q, Ye CP, Jones JE, Elmquist JK, and Lowell BB (2008). Synaptic release of GABA by AgRP neurons is required for normal regulation of energy balance. Nat. Neurosci 11, 998–1000. [PubMed: 19160495]

Wang Q, Liu C, Uchida A, Chuang JC, Walker A, Liu T, Osborne-Lawrence S, Mason BL, Mosher C, Berglund ED, et al. (2013). Arcuate AgRP neurons mediate orexigenic and glucoregulatory actions of ghrelin. Mol. Metab 3, 64–72. [PubMed: 24567905]

Wirkner K, Günther A, Weber M, Guzman SJ, Krause T, Fuchs J, Köles L, Nörenberg W, and Illes P (2007). Modulation of NMDA receptor current in layer V pyramidal neurons of the rat prefrontal cortex by P2Y receptor activation. Cereb. Cortex 17, 621–631. [PubMed: 16648456]

Wu Q, Boyle MP, and Palmiter RD (2009). Loss of GABAergic signaling by AgRP neurons to the parabrachial nucleus leads to starvation. Cell 137, 1225–1234. [PubMed: 19563755]

Wu Z, Kim ER, Sun H, Xu Y, Mangieri LR, Li DP, Pan HL, Xu Y, Arenkiel BR, and Tong Q (2015). GABAergic projections from lateral hypothalamus to paraventricular hypothalamic nucleus promote feeding. J. Neurosci 35, 3312–3318. [PubMed: 25716832]

Xu P, Cao X, He Y, Zhu L, Yang Y, Saito K, Wang C, Yan X, Hinton AO, Jr., Zou F, et al. (2015). Estrogen receptor-α in medial amygdala neurons regulates body weight. J. Clin. Invest 125, 2861–2876. [PubMed: 26098212]

Yang Y, Atasoy D, Su HH, and Sternson SM (2011). Hunger states switch a flip-flop memory circuit via a synaptic AMPK-dependent positive feedback loop. Cell 146, 992–1003. [PubMed: 21925320]

Highlights

- Fasting dramatically diminishes SK3 expression in AgRP/NPY neurons
- Mutation of SK3 in AgRP/NPY neurons increases their activity in the fed state
- Mutation of SK3 in AgRP/NPY neurons facilitates diet-induced obesity
- Mutation of SK3 in AgRP/NPY neurons causes hyperphagia and hypometabolism

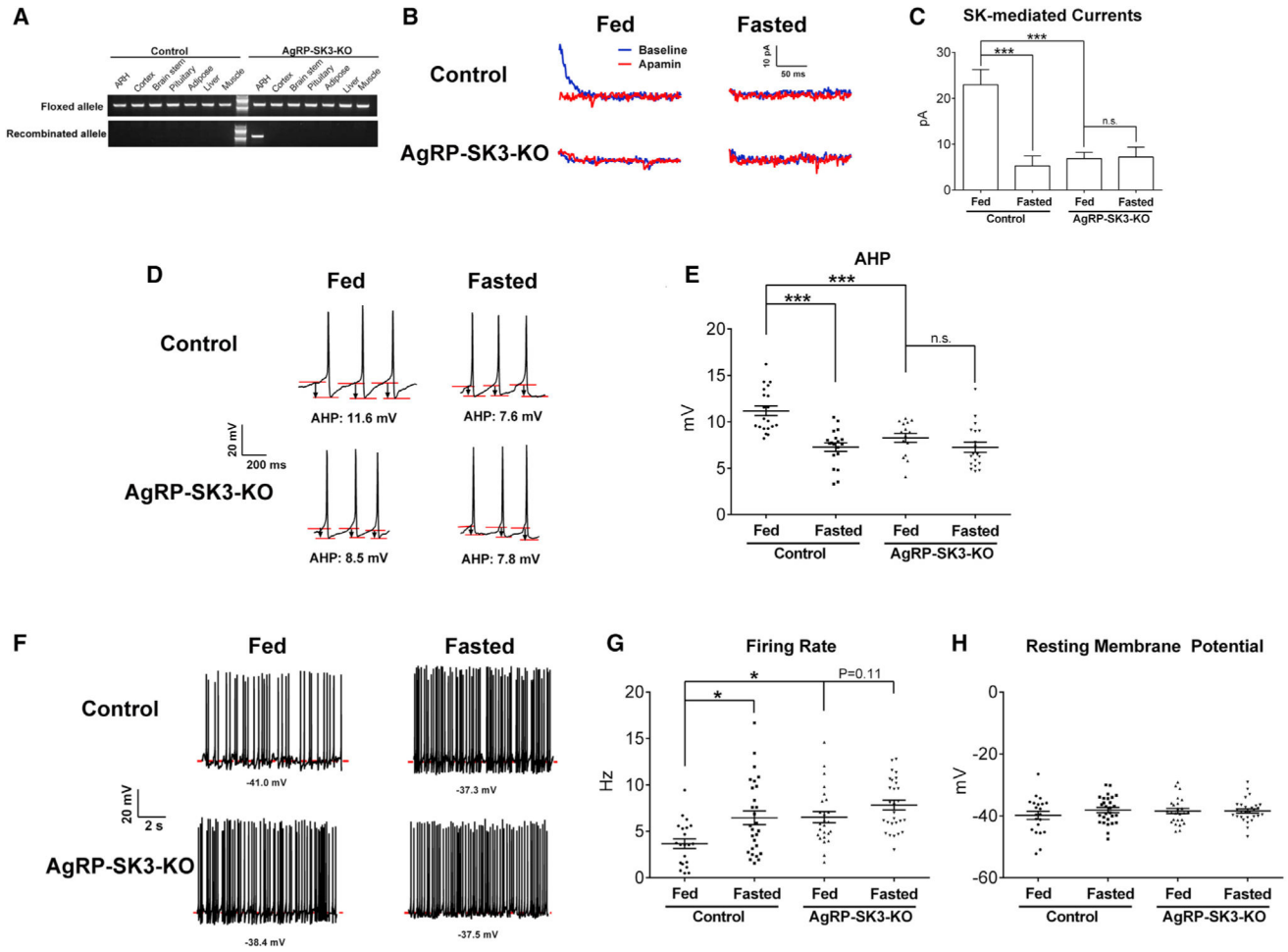

Figure 1. Mutation of SK3 Abolished Feeding-Related Firing Dynamics of AgRP/NPY Neurons

(A) PCR amplification of genomic DNA from various tissues of control (Kcnn3$^{f/f}$) and AgRP-SK3-KO (Kcnn3$^{f/f}$/AgRP-CreERT2) mice. The floxed Kcnn3 allele (643 bp) was detected in all tissues from both mice; the recombined Kcnn3 allele (550 bp) was only detected in AgRP/NPY cell-containing tissues (the ARH).

(B) Representative traces for SK-mediated currents recorded in AgRP/NPY neurons from fed or fasted control or AgRP-SK3-KO mice. Blue traces are baseline SK-mediated currents, and red traces are SK-mediated currents after acute apamin perfusion (100 nM, 6 min).

(C) Quantification showing the amplitude of SK-mediated currents in TOMATO-labeled AgRP/NPY neurons during various conditions. n = 10–40 neurons per condition. Results are shown as mean ± SEM. ***p < 0.001 (two-way ANOVA analyses followed by post hoc Sidak tests).

(D) Three continuous action potentials in AgRP/NPY neurons from fed and fasted control or AgRP-SK3-KO mice; values at the bottom of each trace are amplitudes of the AHP.

(E) Quantification showing the amplitude of the AHP. n = 15–20 neurons per condition. Results are shown as individual data point from each neuron and summarized as mean ± SEM. ***p < 0.001 (two-way ANOVA analyses followed by post hoc Sidak tests).

(F) Representative current clamp traces in AgRP/NPY neurons from fed and fasted control or AgRP-SK3-KO mice.

(G and H) Quantification showing the firing rate (G) and resting membrane potential (H). n = 21–29 neurons per condition. Results are shown as individual data point from each neuron and summarized as mean ± SEM. *$p < 0.05$ (two-way ANOVA analyses followed by post hoc Sidak tests).

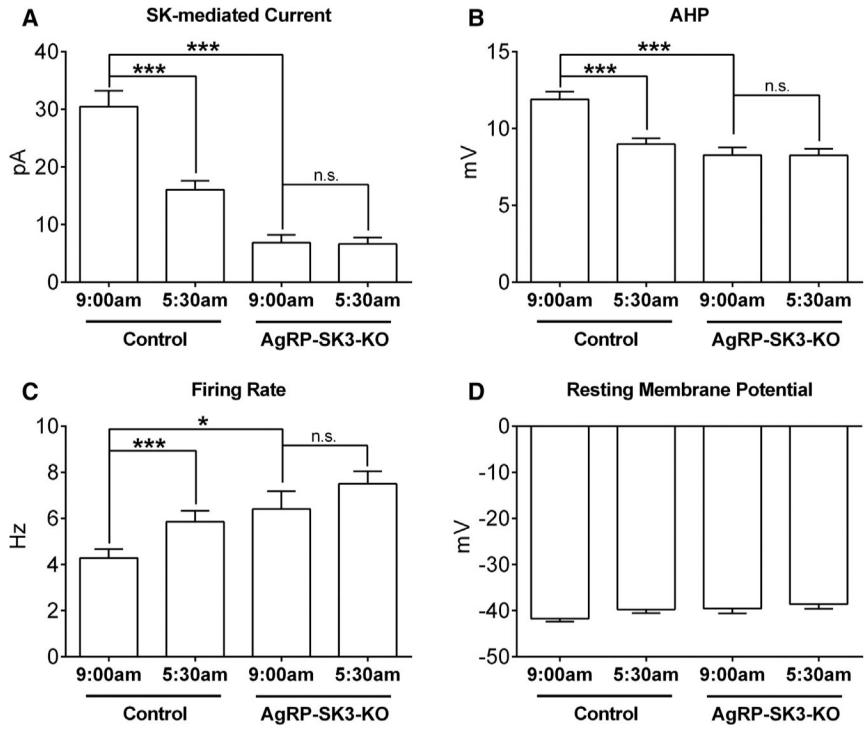

Figure 2. Mutation of SK3 Abolished Circa-dian-Related Firing Dynamics of AgRP/NPY Neurons

(A) The amplitude of SK-mediated currents recorded in AgRP/NPY neurons from ad-libitum-fed control or AgRP-SK3-KO mice at 9 a.m. or at 5:30 p.m. n = 21–40 neurons per condition. Results are shown as mean ± SEM. ***p < 0.001 (two-way ANOVA analyses followed by post hoc Sidak tests).

(B) The amplitude of the AHP in AgRP/NPY neurons from ad-libitum-fed control or AgRP-SK3-KO mice at 9 a.m. or at 5:30 p.m. n = 15–30 neurons per condition. Results are shown as mean ± SEM. ***p < 0.001 (two-way ANOVA analyses followed by post hoc Sidak tests).

(C and D) The firing rate (C) and resting membrane potential (D) in AgRP/NPY neurons from ad-libitum-fed control or AgRP-SK3-KO mice at 9 a.m. or at 5:30 p.m. n = 17–36 neurons per condition. Results are shown as mean ± SEM. *p < 0.05 and ***p < 0.001 (two-way ANOVA analyses followed by post hoc Sidak tests).

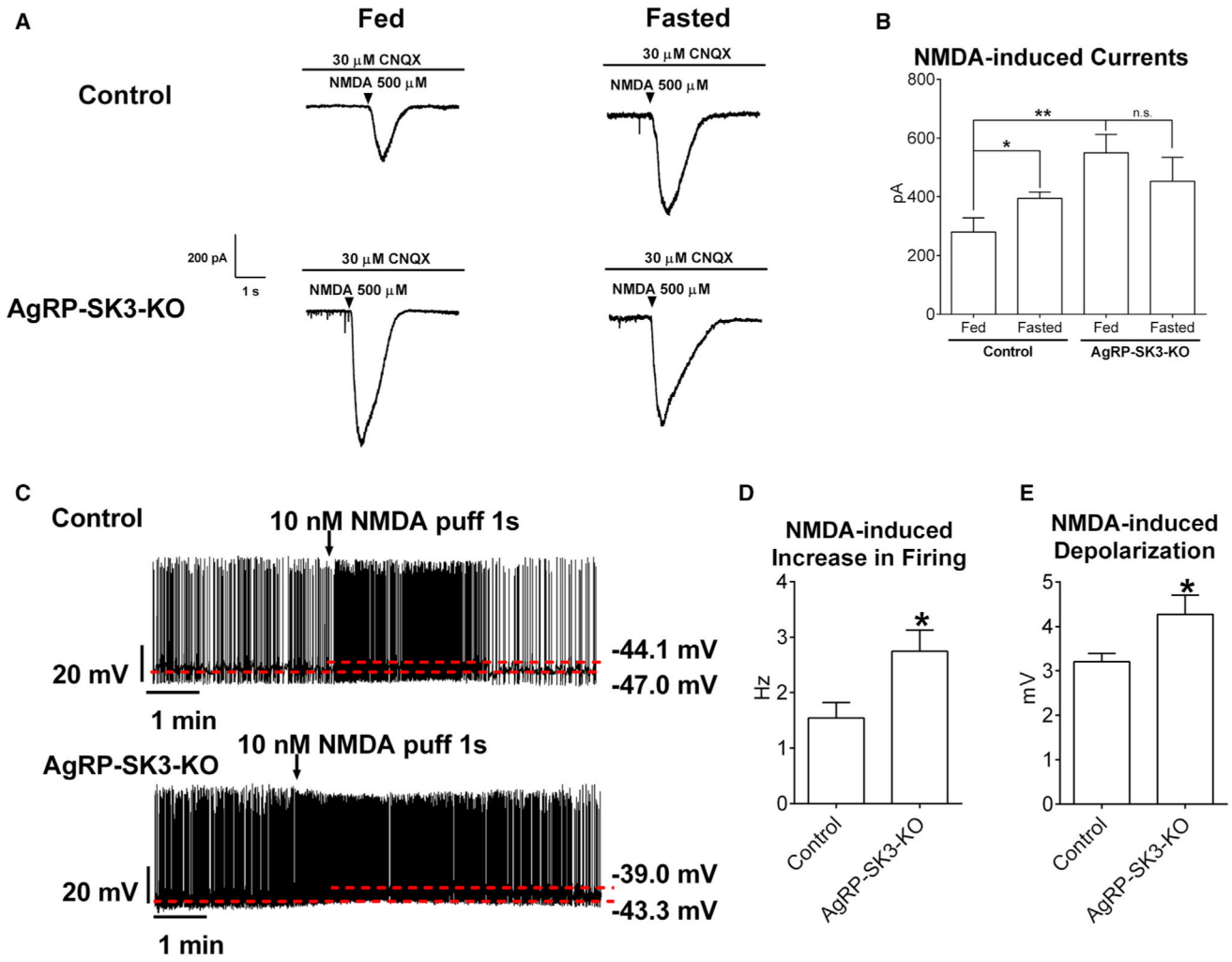

Figure 3. Mutation of SK3 Enhanced NMDA-Induced Activities in AgRP/NPY Neurons

(A) Representative NDMA-induced currents in AgRP/NPY neurons from fed and fasted control or AgRP-SK3-KO mice.

(B) Quantification of NMDA-induced currents. n = 15–22 neurons per condition. Results are shown as mean ± SEM. *p < 0.01 or **p < 0.01 in two way ANOVA analyses followed by post hoc Sidak tests.

(C) Representative current clamp traces in response to NMDA puff in AgRP/NPY neurons from fed control or AgRP-SK3-KO mice.

(D and E) Quantification showing NMDA-induced increases in the firing rate (D) and depolarization (E). n = 13–20 neurons per condition. Results are shown as mean ± SEM. *p < 0.05 (t tests).

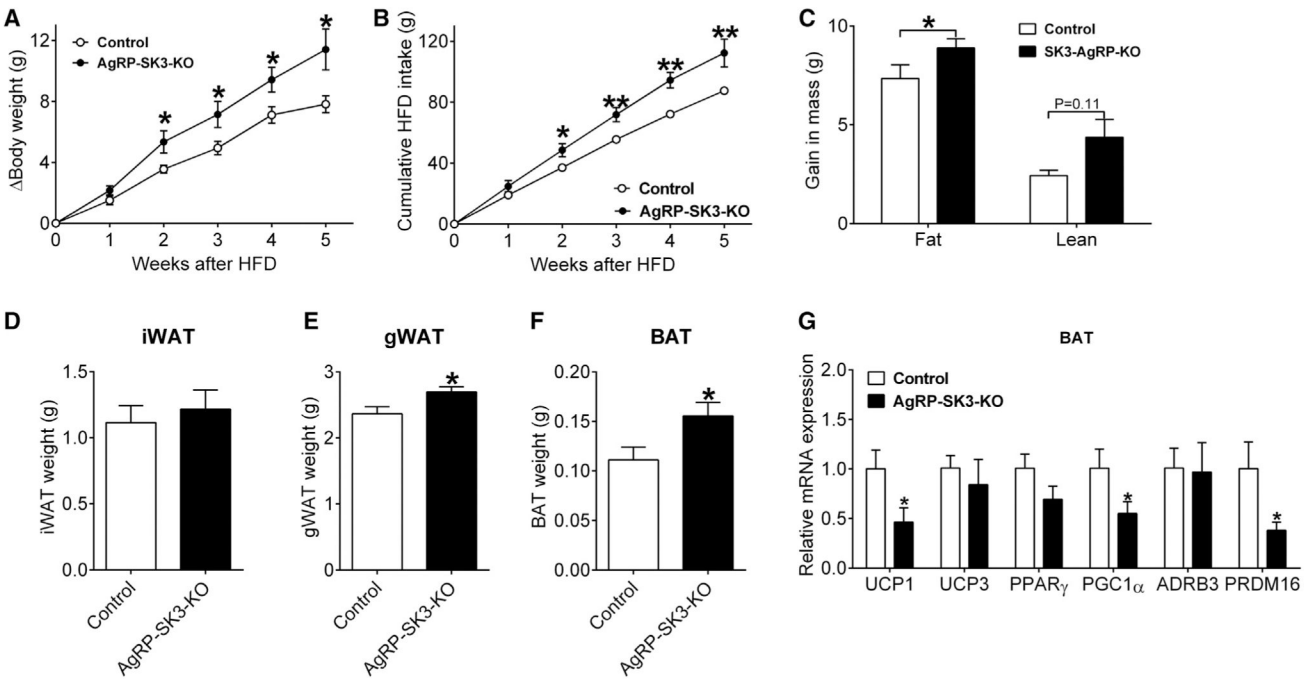

Figure 4. Mutation of SK3 in AgRP/NPY Neurons Increased Susceptibility to DIO

(A) Body weight gain of male control and AgRP-SK3-KO littermates since they were switched to HFD feeding. n = 7 or 9 mice per group. Results are shown as mean ± SEM. *p < 0.05 (t tests for each time point).

(B) Cumulative HFD intake. n = 7 or 9 mice per group. Results are shown as mean ± SEM. *p < 0.05 or **p < 0.01 (t tests for each time point).

(C) Fat mass and lean mass gain since HFD feeding. n = 7 or 11 mice per group. Results are shown as mean ± SEM. *p < 0.05 (t tests for each time point).

(D–F) Weights of iWAT (D), gWAT (E) and BAT (F) pads measured at the end of HFD feeding. n = 7 or 9 mice per group. Results are shown as mean ± SEM. *p < 0.05 (t tests).

(G) Relative mRNA levels of indicated genes in BAT. n = 7 mice per group. Results are shown as mean ± SEM. *p < 0.05 (t tests).

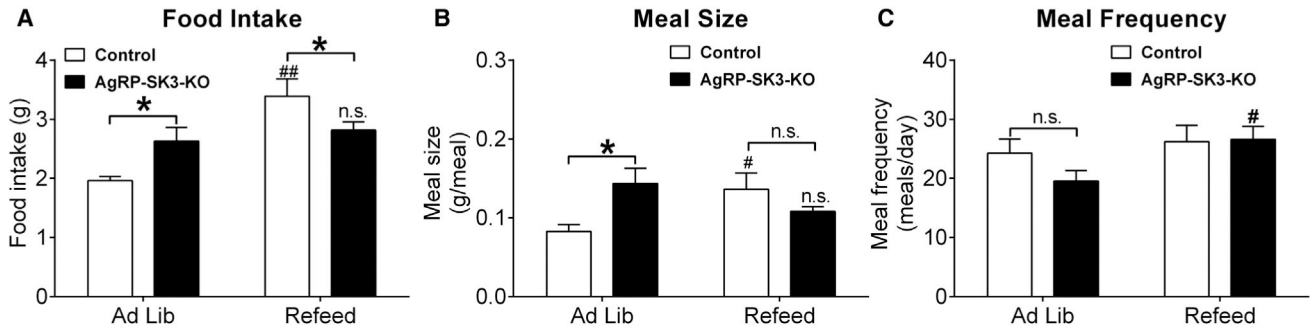

Figure 5. Mutation of SK3 in AgRP/NPY Neurons Caused Abnormal Feeding Behaviors

24-hr food intake (A), meal size (B), and meal frequency (C) during the ad lib or refeeding period. n = 7 mice per group. Results are shown as mean ± SEM. *$p < 0.05$ between control and AgRP-SK3-KO mice within the same period; #$p < 0.05$ or ##$p < 0.01$ between ad libitum and refeed periods of the same mice.

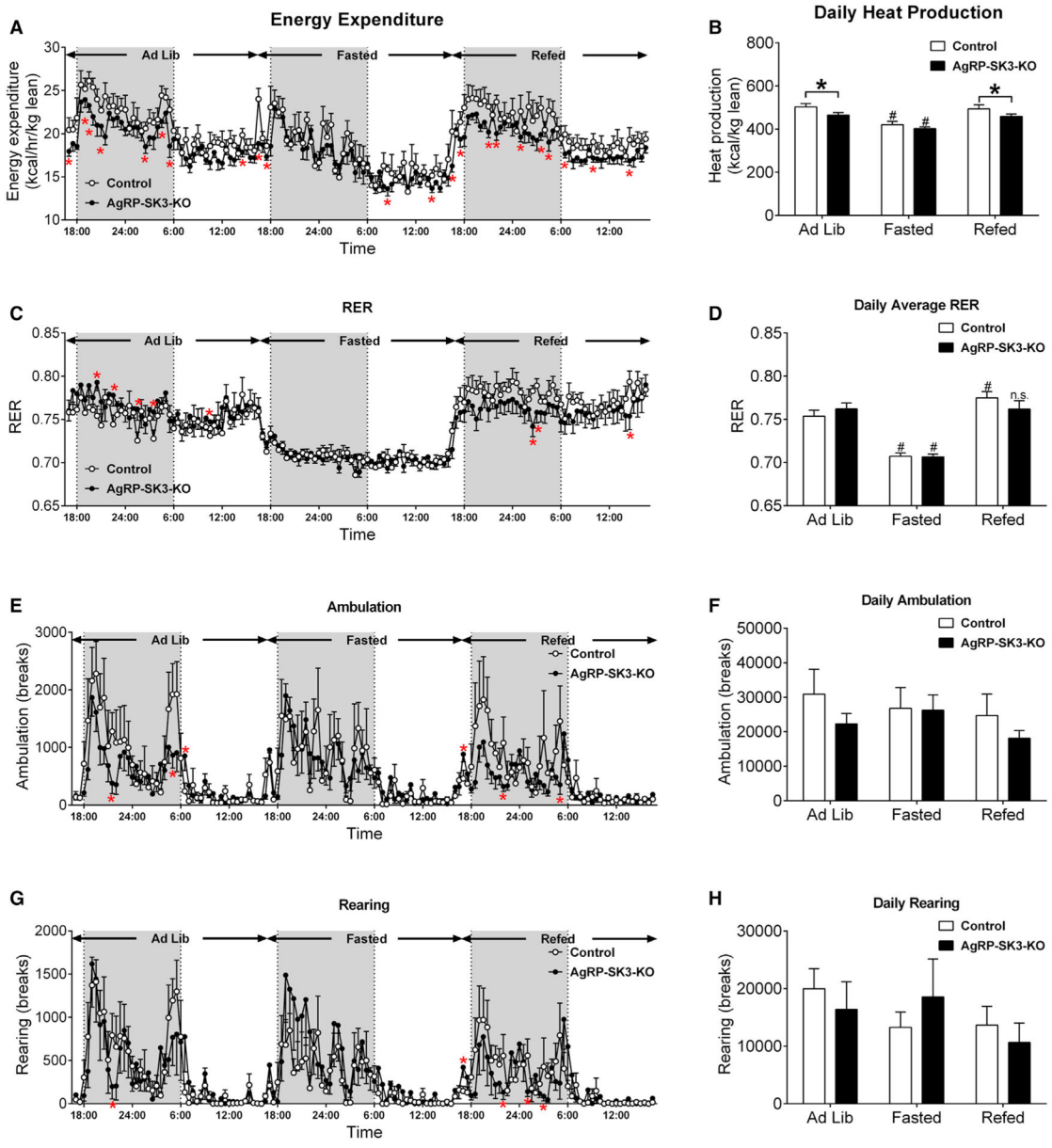

Figure 6. Mutation of SK3 in AgRP/NPY Neurons Decreased Energy Expenditure

(A) Temporal changes in energy expenditure in HFD-fed control and AgRP-SK3-KO mice during a 24-hr ad libitum period, followed by a 24-hr food deprivation and 24-hr refeed period.

(B) Daily energy expenditure calculated from data in (A).

(C) Temporal changes in RER in HFD-fed control and AgRP-SK3-KO mice during a 24-hr ad libitum period, followed by a 24-hr food deprivation and 24-hr refeed period.

(D) Daily averaged RER calculated from data in (C).

(E) Temporal changes in ambulation in HFD-fed control and AgRP-SK3-KO mice during a 24-hr ad libitum period, followed by a 24-hr food deprivation and 24-hr refeed period.

(F) Daily ambulation calculated from data in (E).

(G) Temporal changes in rearing activity in HFD-fed control and AgRP-SK3-KO mice during a 24-hr ad libitum period, followed by a 24-hr food deprivation and 24-hr refeed period.

(H) Daily ambulation calculated from data in (E). n = 7 or 10 mice per group. Results are shown as mean ± SEM. *$p < 0.05$ between control and AgRP-SK3-KO mice at the same time point or within the same period; #$p < 0.05$ versus ad libitum periods of the same mice (two-way ANOVA analyses followed by post hoc Sidak tests).